

**FUSELAGE AERODYNAMICS ANALYSIS THROUGH SEMI
EMPIRICAL METHOD AND COMPUTATIONAL
AERODYNAMICS**

MOHD RIDHWAN BIN ABU BAKAR

A thesis submitted in partial
fulfillment of the requirement for the award of the
Degree of Master of Mechanical Engineering

Faculty of Mechanical Engineering (Manufacturing)
Universiti Tun Hussein Onn Malaysia

MARCH 2014

ABSTRACT

To fulfil the need of civilian and military purposes, there may be more than millions of aircrafts that had been built so far. In year of 2010, The Federal Aviation Administration (FAA) recorded that there were 223,370 aircraft under the category of General Aviation Aircraft is in operation around the world. This type of aircraft serves in the unscheduled flight for various reasons. Other aircrafts which are designed to support scheduled flight used by airlines such as the aircraft produced by aircraft manufacturer such as Boeing, McDonnell Douglas, Airbus, Fokker, Lockheed etc, may already contributed more than 100,000 aircrafts. Strictly speaking hundred thousand aircrafts have already built and each having its own fuselage shape and most of them had been tested under wind tunnel test. Unfortunately, their aerodynamics data kept in a confidential manner by the most aircraft manufacturers. The present work focused on the development of computer code for allowing one to carry out the aerodynamic characteristics over an arbitrary fuselage geometry. The computer code was developed by using semi empirical aerodynamics method in obtaining the overall aerodynamic characteristics and using Three Dimensional Panel Method for their pressure distribution over the fuselage surface. The aerodynamic characteristics analysis was carried out over various shape models and compared with the results provided by DATCOM software. In term of lift and pitching moment coefficient for various angle of attacks, the result of the developed software is in a good agreement with DATCOM software, but totally differ with DATCOM software is in term of drag coefficient. However if the component of base drag is ignored both two computer codes give close results. The effect of cambered fuselage was investigated by modelling the fuselage geometry developed based on NACA series. The result indicates that the maximum camber and the position of the maximum camber give strong influence to the pitching moment. The result of pressure distribution over the fuselage surface indicates that there are significant pressure variation over the body surface due to angle of attack. In addition to this, the research also found that the fuselage nose, fuselage camber line, and fuselage cross section give a strong influence to the overall aerodynamic characteristics.

ABSTRAK

Bagi memenuhi keperluan awam dan tentera, lebih berjuta-juta pesawat telah dibina. Pada tahun 2010, Pentadbiran Penerbangan Persekutuan (FAA), mencatatkan bahawa terdapat 223,370 pesawat udara di bawah kategori Penerbangan Pesawat Umum telah beroperasi di seluruh dunia. Pesawat-pesawat ini dibina mempunyai pelbagai fungsi. Untuk memenuhi permintaan penerbangan, syarikat-syarikat penerbangan seperti Boeing, McDonnell Douglas, Airbus, Fokker, Lockheed dan lain-lain, sudah boleh membina lebih daripada 100,000 pesawat. Terdapat beratus ribu pesawat telah dibangunkan dan setiap satunya mempunyai bentuk fuselaj yang tersendiri dan kebanyakannya telah diuji dengan ujian terowong angin. Malangnya, data aerodinamik disimpan secara sulit oleh setiap pengeluar pesawat. Penyelidikan terkini memberi tumpuan kepada membangunkan kod komputer untuk membolehkan penyelidik lain untuk menjalankan ujian aerodinamik ke atas pelbagai bentuk geometri fuselaj. Kod komputer dibangunkan dengan menggunakan kaedah separuh empirikal aerodinamik bagi mendapatkan ciri-ciri aerodinamik serta menggunakan kaedah Panel Tiga Dimensi untuk mendapatkan taburan tekanan ke atas permukaan fuselaj. Analisis aerodinamik yang dijalankan ke atas pelbagai bentuk model dan hasil kajian tersebut dibandingkan dengan hasil kajian yang diberikan oleh perisian DATCOM. Dalam istilah pekali daya angkat dan momen dalam pelbagai sudut serangan, hasil yang diperolehi amat menghampiri dengan hasil kajian perisian DATCOM, tetapi dari segi pekali seretan, hasil kajiannya memberi perbezaan yang amat ketara. Walaubagaimanapun, jika komponen asas seretan diabaikan, kedua-dua kod komputer memberikan hasil yang hampir antara satu sama yang lain. Kesan fuselaj yang melengkung dikaji dengan kaedah pemodelan geometri fuselaj berasaskan dari NACA. Hasil dari kajian menunjukkan bahawa lengkungan maksimum dan kedudukan maksimum lengkungan memberikan pengaruh yang kuat kepada pekali momen. Hasil taburan tekanan di permukaan badan pesawat menunjukkan bahawa terdapat perubahan tekanan di permukaan badan yang disebabkan oleh sudut serangan amat ketara. Sebagai tambahan, hasil-hasil penyelidikan juga mendapati muncung fuselaj, garis lengkungan fuselaj dan keratan rentas fuselaj memberikan pengaruh yang kuat secara keseluruhan terhadap ciri-ciri aerodinamik.

CONTENTS

| | |
|------------------------------------|-------------|
| TITLE | i |
| DECLARATION | ii |
| ACKNOWLEDGEMENT | iv |
| ABSTRACT | v |
| ABSTRAK | vi |
| CONTENTS | vii |
| LIST OF TABLES | xiii |
| LIST OF FIGURES | xv |
| | |
| CHAPTER I INTRODUCTION | 1 |
| | |
| 1.1 Introduction | 1 |
| 1.2 Research Background | 3 |
| 1.3 Problem Statement | 4 |
| 1.4 Research Objectives | 5 |
| 1.5 Scope of Study | 6 |

| | | |
|-------------------|--|----------|
| CHAPTER II | LITERATURE REVIEW | 7 |
| 2.1 | Introduction | 7 |
| 2.1.1 | Symmetrical Fuselage Model NACA RM L9I30 | 11 |
| 2.1.2 | Symmetrical Fuselage Geometry Model NACA RM A50K24b | 15 |
| 2.1.3 | Symmetrical Fuselage : Agard's Model – 1 | 17 |
| 2.1.4 | Parabolic Spindle Fuselage model | 20 |
| 2.1.5 | Ellipsoid of revolution | 21 |
| 2.2 | Mathematical Model For Generating Symmetrical Fuselages : Multi Segments | 23 |
| 2.2.1 | The Nose Model of NACA RM L53I23A | 26 |
| 2.2.2 | The Nose model of The von Kármán Ogive | 28 |
| 2.2.3 | The Sears-Haack Body | 29 |
| 2.2.4 | Power Law Body | 31 |
| 2.3 | The Unsymmetrical Fuselage Model | 34 |
| 2.3.1 | Unsymmetrical Fuselage Model NACA RM L54K12 | 35 |
| 2.3.2 | Unsymmetrical Fuselage Model Base NACA Series Four Digits | 38 |
| 2.3.3 | Unsymmetrical Fuselage Model Base NACA Series Five Digits | 40 |

| | | |
|--|--|-----------|
| 2.4 | Mathematical Model of Non Circular Fuselage Cross Section | 43 |
| 2.4.1 | Non Circular Fuselage's Cross Section NACA Report TN 4176 | 46 |
| 2.4.2 | Non Circular Fuselage Cross Section of the Fuselage NACA TN 1272 | 49 |
| 2.4.3 | An Aerodynamic Experimental Result of Fuselage with Non Circular Cross Section | 51 |
| 2.5 | Further Development in the Fuselage Design | 57 |
| CHAPTER III METHODOLOGY | | 63 |
| 3.1 | Fuselage's Aerodynamics Semi Empirical Method | 63 |
| 3.2 | Flight Conditions | 71 |
| 3.3 | The Required Parameter of Fuselage Geometry | 73 |
| 3.4 | Digitized Data of Semi Empirical Curve on the Fuselage Aerodynamics Analysis | 76 |
| 3.5 | The Flowchart of the aerodynamics analysis for Fuselage Model | 80 |
| CHAPTER IV DISCUSSION & RESULT | | 82 |
| 4.1 | The Developed Computer Code | 82 |
| 4.2 | Computer Code Validation | 83 |

| | | |
|-----------------------------|---|------------|
| 4.2.1 | Fuselage model of DATCOM Handbook | 83 |
| 4.3 | Comparison Result With DATCOM Handbook In Term Of Pitching Moment Coefficient | 90 |
| 4.4 | Effect Of Number Division Fuselage Sections | 92 |
| 4.5 | Comparison Result With DATCOM Software | 93 |
| 4.6 | The Problem on the Drag Coefficient Calculation | 96 |
| 4.7 | Comparison Aerodynamics Characteristics Over Various Fuselage Models | 102 |
| 4.8 | The Fuselage Model Of Non Circular Cross Section | 107 |
| 4.9 | The Cambered Fuselage Model | 116 |
| 4.10 | The Computational Aerodynamics Analysis | 133 |
| CHAPTER V CONCLUSION | | 137 |
| 5.1 | Conclusion | 137 |
| REFERENCES | | 140 |
| APPENDIX | | 145 |

LIST OF TABLES

| | | |
|-------|---|----|
| 2.1 | Distribution of fuselage diameter of the fuselage NACA RM L54KL2 | 10 |
| 2.2 | Parameter fuselage geometry of fuselage model NACA RM 19I30 | 12 |
| 2.3 | The List of NACA Report adopted Fuselage Model RM A50K24b | 15 |
| 2.4 | The actual fuselage length of RM-10 missile related with the size of wind tunnel test section | 19 |
| 2.5 | Nose ordinates of AGARD Model 2 | 24 |
| 2.6 | Basic ordinates of Symmetrical Fuselage RM L54K12 | 35 |
| 2.7 | Basic ordinates of Unsymmetrical Fuselage RM L54K12 | 36 |
| 2.8 | The required values of parameter for the NACA series 5 digits with $Q=0$ | 41 |
| 2.9 | The required values of parameter for the NACA series 5 digits with $Q=1$ | 42 |
| 2.10a | The Distribution of the radius fuselage cross section of NACA TN 4176 | 48 |

| | | |
|-------|---|-----|
| 2.10b | The Distribution of data rectangular cross section NACA TN 4176 | 48 |
| 2.11 | The parameter geometry of the fuselage NACA TN 1272 | 50 |
| 2.12 | The parameter geometry of the fuselage NACA Rep 540 | 51 |
| 2.13 | The Distribution of the radius of fuselage cross section along the longitudinal x-axis | 52 |
| 2.14 | Length and aircraft width of various type aircrafts | 60 |
| 3.1 | Digital Data of the graph of apparent mass factor (K_2-K_1) as function of fineness ratio FNR | 77 |
| 3.2 | The graph of the ratio drag coefficient η as function of fineness ratio FNR | 78 |
| 3.3 | The graph of the Steady State Cross Flow Drag Coefficient as function of $M^\infty \sin \alpha$ | 79 |
| 4.1 | Distribution fuselage width and height | 86 |
| 4.2 | Parameter Geometry Fuselage of DATCOM Model | 88 |
| 4.3 | The required values of parameter for the NACA series 5 digits with $Q=0$ | 118 |
| 4.4 | The required values of parameter for the NACA series 5 digits with $Q=1$ | 118 |
| 4.5 | The aerodynamics characteristics two dimensional model at zero lift angle of attack | 129 |

LIST OF FIGURES

| | | |
|------|---|----|
| 2.1 | The definition of symmetrical and unsymmetrical fuselage shape | 9 |
| 2.2 | Fuselage model RML9I30-1 Fineness ratio $F_N = 12.5$, with (a) $X_M = 0.2L$. (b) $X_M = 0.4L$, (c) $X_M = 0.6L$ and (d) $X_M = 0.8L$ | 13 |
| 2.3 | Fuselage RML9I30-1 with position maximum diameter $X_M = 0.6L$ and different Fineness ratio. (a) $F_N = 12.5$, (b) $F_N = 8.91$ and (c) $F_N = 6.04$ | 15 |
| 2.4 | The top view of wing body configuration with fuselage shape according to Eq. 2.2 | 15 |
| 2.5 | Fuselage Model RM A50K24b | 17 |
| 2.6 | The Tail Body Configuration of AGARD Model | 18 |
| 2.7 | Agard Fuselage Model (a) Fuselage length $L_B = 50$ inc and (b) $L_B = 7.325$ inches | 19 |
| 2.8 | Parabolic Spindle Fuselage Model (a) Fineness ratio $F_N = 5$, (b) $F_N = 10$ | 21 |
| 2.9 | Ellipsoidal Fuselage Model (a) Fineness ratio $F_N = 5$, (b) $F_N = 10$ | 22 |
| 2.10 | Basic Dimension of AGARD Model – B | 23 |
| 2.11 | Fuselage of Agard Model – 2 (a), Fuselage nose length $3D$, (b) Fuselage nose length $5D$ | 25 |

| | | |
|-------|--|----|
| 2.12 | The first Group of Nose Model of Fuselage Model NACA RM L53I23A | 26 |
| 2.13 | The Second Group of Nose Model of Fuselage Model NACA RM L53I23A | 27 |
| 2.14 | The Third Group of Nose Model of Fuselage Model NACA RM L53I23A | 27 |
| 2.15 | Two sections fuselage with the Von Karman nose model | 29 |
| 2.16 | Fuselage model with Sears Haack Nose geometry | 31 |
| 2.17 | Fuselage with Power law body model for the nose part. (a) $m = 0.25$, (b) $m = 0.50$, (c) $m = 0.75$ (d) $m = 0.9$ | 33 |
| 2.18 | Some examples of aircraft with unsymmetrical fuselage | 35 |
| 2.19 | Symmetrical and Unsymmetrical Fuselage of RM L52K24's Fuselage model | 38 |
| 2.20 | Symmetrical (a) and unsymmetrical fuselage (b) based on airfoil NACA Series 4 Digits NACA 4415 | 40 |
| 2.21 | Unsymmetrical fuselage based on airfoil NACA 5 digits (a) NACA 23015 and (b) NACA 2311 | 43 |
| 2.22a | Ellipse cross sectional shape | 44 |
| 2.22b | Circular cross sectional shape | 44 |
| 2.22c | Linear side wall cross sectional shape | 45 |
| 2.22d | A cusped or chine-like shape cross sectional shape | 45 |
| 2.22e | A nearly rectangular fuselage cross section | 45 |

| | | |
|-------|--|----|
| 2.23 | Cross-section for various values of n | 46 |
| 2.24 | Side view of fuselage model NACA TN 4176 | 47 |
| 2.25 | The shape of Fuselage cross section of NACA TN 4176 | 47 |
| 2.26a | Triangular Cross Section fuselage model NACA TN 1272 | 49 |
| 2.26b | Elliptical Cross Section fuselage model NACA TN 1272 | 49 |
| 2.27 | Side view of four fuselage model NACA TN 3551 | 52 |
| 2.28a | The Definition of Parameter for Square Fuselage Cross Section | 53 |
| 2.28b | The Definition of Parameter for Rectangular Fuselage Cross Section | 53 |
| 2.29a | The Aerodynamics experiment results of four fuselage models with center of gravity of the model at $\frac{1}{4} C_{mac}$ of unswept wing | 55 |
| 2.29b | The Aerodynamics experimental result of four fuselage models with center of gravity of the model at $\frac{1}{4} C_{mac}$ of swept wing | 56 |
| 2.30 | The CAD model of the ANSAT helicopter | 58 |
| 2.31 | The surface mesh of the ANSAT Helicopter model | 58 |
| 2.32 | The contour of pressure coefficient distribution over the body surface | 59 |
| 2.33 | Aircraft Cross Section in corresponding with passenger seating | 61 |
| 2.34 | The close up of mesh flow domain of the fuselage of LSA Vampire | 62 |
| 2.35 | Pressure distribution in the flow field and body surface of LSA Vampire | 62 |

| | | |
|-----|---|----|
| 3.1 | Coordinate System for Fuselage Aerodynamic Analysis | 64 |
| 3.2 | Apparent Mass Factor (k_2-k_1) | 68 |
| 3.3 | Body Station Where the Flow Becomes Viscous | 68 |
| 3.4 | Ratio of Drag Coefficient of A Circular Cylinder of Finite Length to that of A Cylinder Infinite Length | 69 |
| 3.5 | Steady State Cross Flow Drag Coefficient for Circular Cylinder | 69 |
| 3.6 | Turbulent mean skin friction coefficient on an insulated plate | 70 |
| 3.7 | The GETDATA Graph Digitizer Software's shoot screen | 76 |
| 3.8 | Flow chart of the Developed Computer Code | 81 |
| 4.1 | Fuselage Geometry of DATCOM Handbook | 83 |
| 4.2 | Comparison result of Pitching Moment Coefficient between Present Computer Code and DATCOM Handbook | 91 |
| 4.3 | Comparison result of Pitching Moment Coefficient between Present Computer Code and DATCOM Handbook for the Case of 20 Fuselage Segments | 92 |
| 4.4 | Comparison result of Pitching Moment Coefficient between Present Computer Code and DATCOM Handbook for the Case of 60 Fuselage Segments | 93 |
| 4.5 | Comparison Result Lift Coefficient C_L Between DATCOM Software and Present Code | 95 |
| 4.6 | Comparison Result Pitching Moment Coefficient C_M Between DATCOM Software and Present Code | 95 |
| 4.7 | Comparison Result Drag Coefficient C_D between Drag Method – 1 and Drag Method – 2 Produced by the Present Code | 96 |

| | | |
|-------|--|-----|
| 4.8 | The Percentages of the Component of Drag Coefficient Due to Lift with Respect to the Zero Lift Drag Coefficients for the Drag Method – 1 | 97 |
| 4.9 | The Percentages Differences of the Component of Drag Coefficient Due to Lift with Respect to the Zero Lift Drag Coefficient | 98 |
| 4.10 | Comparison Result Drag Coefficient C_D between Drag Method – 1 and DATCOM Software Produced by Present Code | 98 |
| 4.11 | Comparison result of Drag Coefficient Between DATCOM Software and the Modified Present Computer Code | 101 |
| 4.12 | Comparison of fuselage shape in nose | 103 |
| 4.13 | Comparison Results of Lift Coefficient over Various Shape of Fuselage | 104 |
| 4.14 | Comparison Results of Pitching Moment Coefficient over Various Shape of Fuselage | 105 |
| 4.15 | Comparison Results of Drag Coefficient over Various Shape of Fuselages | 106 |
| 4.16 | Side view of the actual airplane Lockheed Three Stars L-1011 | 107 |
| 4.17 | The variation fuselage cross section of the Airplane Lockheed Three Stars L-1011 | 108 |
| 4.18 | The variation fuselage cross section of the NASA Airplane – A | 109 |
| 4.19a | Rectangular Cross section fuselage width > fuselage height | 110 |
| 4.19b | Rectangular Cross section fuselage width > fuselage height | 110 |

| | | |
|-------|---|-----|
| 4.19c | Rectangular Cross section fuselage width > fuselage height | 111 |
| 4.20a | Fuselage geometry with circular cross section | 111 |
| 4.20b | Fuselage geometry with squarer cross section | 112 |
| 4.20c | Fuselage geometry with rectangular cross section , Fuselage width less than fuselage height | 112 |
| 4.20d | Fuselage geometry with rectangular cross section, fuselage width greater than fuselage height | 113 |
| 4.21a | A comparison result of lift coefficient C_L between DATCOM Software and the Present Code for different fuselage cross sections | 113 |
| 4.21b | A comparison result of pitching moment coefficient C_M between DATCOM Software and the Present Code for different fuselage cross sections | 114 |
| 4.21c | A comparison result of Drag coefficient C_D between DATCOM Software and the Present Code for different fuselage cross sections | 115 |
| 4.22 | The side view of NASA aircraft model | 116 |
| 4.23 | The shape of camber line for NACA series 4 Digits for different values of maximum camber setting at a fixed position maximum camber $x_{ycmax} = 0.1 c$ | 121 |
| 4.24 | The shape of camber line for NACA series 4 Digits for different values of maximum camber setting at a fixed position maximum camber $x_{ycmax} = 0.5 c$ | 121 |

| | | |
|-------|--|-----|
| 4.25 | Shape camber line's NACA 4 digits with different position maximum thickness | 122 |
| 4.26a | Distribution camber NACA series 5 Digits for model 210., 220., 230., 240., 250... | 122 |
| 4.26b | Distribution camber NACA series 5 Digits for model 211., 221..., 231..., 241..., 251... | 123 |
| 4.27 | Distribution camber of NACA series 6 digit standard for different lift coefficient design | 123 |
| 4.28a | Lift Coefficient NACA series 4 Digit varying position of maximum camber. The maximum camber $Y_{cmax} = 0.01 c$ | 124 |
| 4.28b | Profile Drag Coefficient NACA series 4 Digit varying position of maximum camber. The maximum camber $Y_{cmax} = 0.01 c$ | 125 |
| 4.28c | Pitching Moment Coefficient NACA series 4 Digit varying position of maximum camber. The maximum camber $Y_{cmax} = 0.01 c$ | 125 |
| 4.29a | Lift Coefficient NACA series 4 Digit varying position of maximum camber. The maximum camber $Y_{cmax} = 0.02$ | 126 |
| 4.29b | Profile Drag Coefficient NACA series 4 Digit varying position of maximum camber. The maximum camber $Y_{cmax} = 0.02 c$ | 126 |
| 4.29c | Profile Drag Coefficient NACA series 4 Digit varying position of maximum camber. The maximum camber $Y_{cmax} = 0.02 c$ | 127 |
| 4.30a | Lift Coefficient NACA series 4 Digit varying position of maximum camber. The maximum camber $Y_{cmax} = 0.05 c$ | 127 |

| | | |
|-------|--|-----|
| 4.30b | Profile Drag Coefficient NACA series 4 Digit varying position of maximum camber. The maximum camber $Y_{cmax} = 0.05 c$ | 128 |
| 4.30c | Pitching Moment Coefficient NACA series 4 Digit varying position of maximum camber. The maximum camber $Y_{cmax} = 0.05 c$ | 128 |
| 4.31a | The zero lift angle of attack variation due to camber line for NACA series 4 digits | 131 |
| 4.31b | The drag coefficient at zero lift angle of attack variation due to camber line for NACA series 4 digits | 131 |
| 4.31c | The drag coefficient at zero lift angle of attack variation due to camber line for NACA series 4 digits | 132 |
| 4.32a | The pressure coefficient distribution at different meridian angle at angle of attack $\alpha = 0$, Upper half fuselage side | 133 |
| 4.32b | The pressure coefficient distribution at different meridian angle at angle of attack $\alpha = 0$, Lower half fuselage side | 134 |
| 4.33a | The pressure coefficient distribution at different meridian angle at angle of attack $\alpha = 3$, Upper half fuselage side | 135 |
| 4.33b | The pressure coefficient distribution at different meridian angle at angle of attack $\alpha = 3$, Lower half fuselage side | 136 |

CHAPTER I

INTRODUCTION

1.1 Introduction

The fuselage, or body of the airplane represents a long hollow tube which holds all the pieces of aircraft components together. The fuselage is designed as a hollow tube to reduce weight. Conventionally the role of fuselage is carrying passengers. Besides that, fuselages are also designed to accommodate antennas, oversized cargo, and any sort of devices according to what the aircraft is intended to. The aircraft fuselage is basically responsible for 25-50 percent of the overall drag for most airplanes. Fuselages generates the following types of drag; profile drag, compressibility drag, and induced drag. A fuselage contributes to induced drag primarily because its adverse effect on wings span load distribution. When the fuselage is integrated into the wing (and with nacelles and the empennage), extra drag, the so called interference drag is produced. Many aerospace design teams frequently treat fuselage aerodynamic design as a matter of secondary importance during the aircraft development phases. Understandably, aerodynamicists prefer to focus their efforts on wing design employing inverse or optimization methods in order to obtain, for example, transonic wings with minimum wave drag. Usually, fuselage aerodynamic design is scheduled for the last stage of the development phase. At this point, time

is a major issue and as far as the multidisciplinary aspects of fuselage aerodynamics is concerned, a less elaborated work is then performed. It is worth mentioning that the drag creep of a well-designed wing should be under 10 drag counts ($CD = 0.001$) at maximum cruise condition. Drag resulting from a poor fuselage design is likely to overcome such figure due to small separations, shock waves, or excess wetted area. There is also a significant impact on other aircraft regions because disturbed airflow can contribute to lower efficiency of engine inlets and tail surfaces. Separated airflow arising at wing-fuselage junction or fuselage regions has a similar behaviour to vortex shedding from wings. Thus, the disturbed air pattern is prone to cause earlier-than-anticipated fatigue on tail surface structural parts. Frequently, this phenomenon is difficult to diagnose. Considering that it is desirable to have as little drag as possible, the fuselage should be sized and shaped accordingly. Basically there are some factors need to be accounted in designing the fuselage, such as ^[48]:

- Low aerodynamic drag.
- Minimum aerodynamic instability.
- Comfort and attractiveness in terms of seat design, placement, and storage space.
- Safety during emergencies such as fires, cabin depressurization, ditching, and proper placement of emergency exits, oxygen systems, etc.
- Ease of cargo handling in loading and unloading, safe and robust cargo hatches and doors.
- Structural support for wing and tail forces acting in flight, as well as for landing and ground operation forces.
- Structural optimization to save weight while incorporating protection against corrosion and fatigue.
- Flight deck optimization to reduce pilot workload and protect against crew fatigue and intrusion by passengers.
- Convenience, size, and placement of galleys, lavatories, and coat racks.
- Minimization of noise and control of all sounds so as to provide a comfortable and secure environment.
- Climate control within the fuselage including air conditioning, heating, and ventilation.

- Provision for housing a number of different sub-systems required by the aircraft, including auxiliary power units, hydraulic system, air conditioning system, etc.

Most aircrafts were designed with the combination of above factors and they were built with the use of unsymmetrical fuselage shape. This situation was also applied to the aircraft which was designed to be a platform for unmanned aerial vehicles. The unsymmetrical fuselage made the zero lift angle of attack will not occur at zero angle of attack, but at any angle of attack depending on the shape of fuselage camber line. The aerodynamics analysis method applied to the case of a symmetrical fuselage can be adopted for the analysis of unsymmetrical fuselage as far as the zero lift angle of attack for the corresponding fuselage is known. Unfortunately the manner in how to define this zero lift angle of attack was not yet established. Wolowicz et.al. used graphical approach in order to define the zero lift angle of attack $\alpha_{L=0}$ as reported in Ref. 3. While the DATCOM book^[1, 2] did not discuss the way to determine the angle, but their software provide the ability to predict the aerodynamics characteristics for unsymmetrical fuselage.

1.2 Research Background

In parallel of the advancement of computer technology, material, propulsion system and better understanding on the aircraft stability had made the development of autonomous flying vehicle becomes an attracted matter. This type of flying vehicle called Autonomous Aerial Vehicle (UAV) offers various useful applications both in military point of view as well as in civilian's activity.

In view of military application, the UAV can be used as:

1. Reconnaissance surveillance and Target acquisition (RSTA).
2. Surveillance for peacetime and combat synthetic aperture radar (SAR).
3. Deception operations.

4. Maritime operations (Naval fire support, over the horizon targeting, anti-ship missile defence, ship classification).
5. Electronic warfare (EW) and SIGINT (SIGnals INTTelligence).
6. Special and psyops.
7. Meteorology missions.

UAV is designed as an aircraft without pilot which gives it relatively smaller size compared to the size of ordinary manned flying vehicles. The airframe UAV was designed just to fulfil the required payload, fuel and its onboard flight control system. To fulfil such requirements, the UAV's fuselage was not as a symmetrical body but slightly in the form of arbitrary shape. Unfortunately, for every flying vehicle designed to fly on its own flight control system required a precise aerodynamics characteristics data. For UAV, fuselage may give a strong aerodynamics influence to the overall aerodynamics characteristics of the aircraft. Hence, an accurate fuselage aerodynamics analysis is needed for the success of designing a flight control system of the UAV. The present work focused on the development of aerodynamics analysis computer code based on semi empirical aerodynamic method for an arbitrary fuselage shape.

1.3 Problem Statements

Fuselage plays an important role in any type of aircraft. This aircraft component represent the part which all other aircraft components will be attached. The size and shape of fuselage may depend on the payload and also the aircraft engine placements. As a result, the fuselage may contribute around 25 % to 50 % ^[37] of the total drag force on the airplane depending on the shape and size of the fuselage. The best fuselage design contributes the smallest drag without an excessive pitching moment. In addition to this one might expect the presence of lift although the angle of attack is zero. Such condition can be achieved if the fuselage designed as cambered fuselage. To obtain the most suitable fuselage one need an appropriate fuselage aerodynamics analysis software capable for predicting the aerodynamics characteristics of symmetrical as well as unsymmetrical fuselage shape.

1.4 Research Objectives

To develop the aerodynamic capability in predicting the fuselage aerodynamic characteristics which may be useful for designing flying vehicles such as light aircraft, UAV or missile, the research objectives will be carried out involve :

1. Creating the data base for various symmetrical fuselage models based on their shapes defined by a single component or two components consist of nose and mid body.
2. Developing computer code which allow one to visualize the fuselage shape in three dimensional view by using Tecplot software
3. Developing computer code based on given fuselage geometry to generate set of data needed in carrying out the aerodynamic analysis by using DATCOM software.
4. Developing computer code to analyse various fuselage geometry with better fuselage representations compared to the DATCOM software.
5. To investigate the aerodynamic characteristics of various fuselage shapes by using the developed computer code.
6. Developing computer code for predicting the pressure distribution over a symmetrical fuselage model by using Three Dimensional Panel Method.

1.5 Scope of Study

As mentioned in the previous sub chapter, the contribution of the fuselage aerodynamics characteristics to the overall aerodynamics characteristics of the aircraft need to be estimated precisely in the aircraft design work. An accurate aerodynamics characteristics prediction result

becoming more important if one want to success in the development of flight control system. There are three approaches which can be done to estimate the fuselage aerodynamics. They are namely by using of (1) aerodynamics semi empirical method such as DATCOM, (2) Computational Aerodynamics/ Computational Fluid Dynamics and (3) Experimental aerodynamics by using wind tunnel. The present work will deal with the first two approaches and in context with the objectives of the research work as mentioned above, the scope of study in this research work involves:

1. The study on various fuselage geometry from fuselage consist as a single to multi components.
2. Study on various fuselage nose models commonly use in the designing flying vehicles.
3. Study on the use of post processing software for three dimensional plotting fuselage geometry by use Tecplot and DATCOM software for their aerodynamics analysis.
4. Study on the aerodynamics analysis for symmetrical and unsymmetrical fuselage based on semi empirical aerodynamics method.
5. Study on the implementation of Panel Method for Fuselage aerodynamics analysis.

CHAPTER II

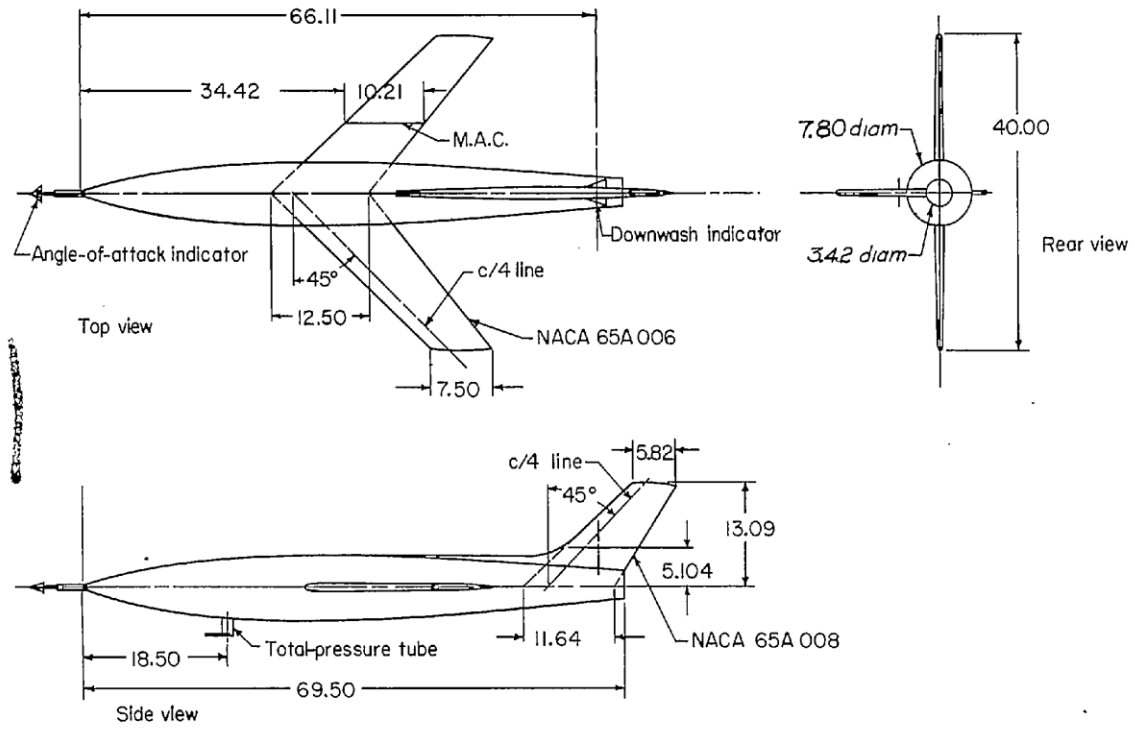
LITERATURE REVIEW

2.1 Introduction

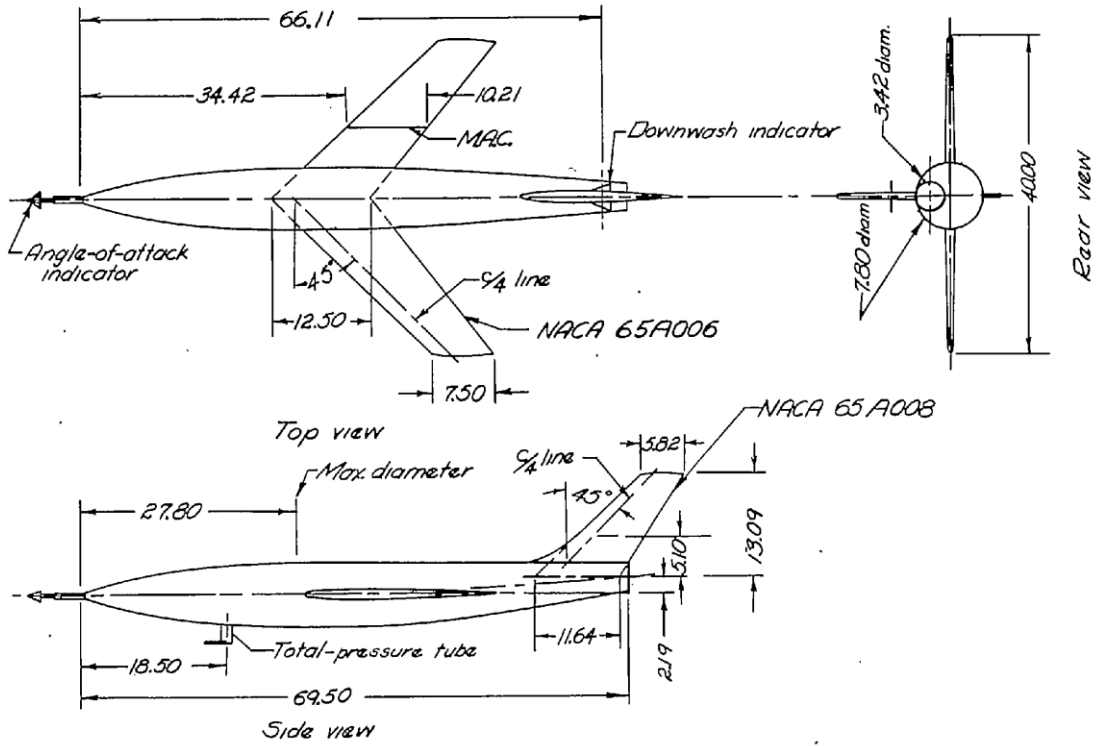
The success of two Wright brothers making the first flight in 1903, had open up the opportunity for various countries to develop the aircraft technology. As a result, more than million aircrafts had been built and flown. Various type of aircraft had been introduced and the aircraft can be classified into several manners. The aircraft can be classified for instance according to the method how the aerodynamic lift force created. This point of view give the aircraft can be classified as a fixed wing aircraft and rotary wing aircraft.

Other classification of the aircraft may be from the point of view of their flight characteristic. From the range capability, the aircraft can be classified as a short, medium or long range aircraft. From the capability in takeoff and landing, the aircraft can be classified as a vertical takeoff and landing (VTOL) aircraft, or a short takeoff and landing (STOL) aircraft as opposed to the aircraft which having a normal takeoff and landing capability. The further aircraft classification may be derived from the type and the number of engine used or based on the shape of wing plan form or also according to how the arrangement of the aircraft components. So, here one can recognize the presence of the type of aircraft belong to the class of low wing aircraft,

high wing or mid wing aircraft. While from the aircraft tail configuration one can identify the aircraft belong to the T tail aircraft or V tail aircraft. Every class or category of the aircraft will give influence to the fuselage shape of the corresponding aircraft. As result, there are variety of fuselage shape. The number of fuselage variety may have the same number of variety aircraft that had been built so far. However for stand point aerodynamics characteristics, the fuselage shape can be grouped into two. They are namely a symmetrical and unsymmetrical fuselage. To distinguish between them, the present work uses the definition according to Parks^[4]. In the three dimensional views for a given aircraft drawing in top view, side view and rear view as depicted in the Figure 2.1. The fuselage shown in this figure has a circular cross section uniformly distributed along the longitudinal axis. The center of cross section at each fuselage station coincided with longitudinal axis resulted the aircraft seen from a rear side, the center of cross section at each fuselage station looks as a single points. Such fuselage shape is called as a symmetrical fuselage. In defining the unsymmetrical fuselage, Parks made a modification to the symmetrical fuselage. He made the part of upper fuselage surface rearward of the maximum diameter station parallel to the original fuselage center line and retaining the original fuselage coordinates in planes normal to it. This approach gives the unsymmetrical fuselage in three dimensional views as shown in the Figure 2.2.



(a) Symmetric fuselage model.



(b) Unsymmetric fuselage model.

Figure 2.1: The definition of symmetrical and unsymmetrical fuselage shape^[4]

The symmetrical fuselage as presented in Figure 2.1 represents a parabolic body of revolution of fineness ratio 8.91 with maximum thickness at 40 % of the length. Fuselage ordinates are given in tabulated form as in Table 2.1

Table 2.1: Distribution of fuselage diameter of the fuselage NACA RM L54KL2^[4]

| No | Fuselage Station x (inch) | Fuselage diameter D (inch) |
|----|---------------------------|----------------------------|
| 1 | 0 | 0.0 |
| 2 | 3 | 1.60 |
| 3 | 6 | 3.00 |
| 4 | 9 | 4.24 |
| 5 | 12 | 5.28 |
| 6 | 15 | 6.14 |
| 7 | 18 | 6.84 |
| 8 | 21 | 7.34 |
| 9 | 24 | 7.66 |
| 10 | 27.8 | 7.80 |
| 11 | 30 | 7.78 |
| 12 | 33 | 7.74 |
| 13 | 36 | 7.64 |
| 14 | 39 | 7.48 |
| 15 | 42 | 7.30 |
| 16 | 45 | 7.06 |
| 17 | 48 | 6.78 |
| 18 | 51 | 6.44 |
| 19 | 54 | 6.08 |
| 20 | 57 | 5.66 |
| 21 | 60 | 5.18 |
| 22 | 63 | 4.68 |
| 23 | 66 | 4.12 |
| 24 | 69.5 | 3.42 |

As result of the aircraft technology requirement and development, there are various type of fuselage that had been introduced and implemented in designing a new flying vehicle. The required fuselage may represent a fuselage with three sections: nose, fuselage mid section and the fuselage tail cone. While other may came in the form of fuselage with two sections: fuselage nose and the fuselage mid section. In addition to this, there are some fuselages without clear partition in respect of those parts.

Several example of mathematical models can be used to generate a symmetrical fuselage in the form of single segment for instances:

2.1.1 Symmetrical Fuselage Model NACA RM L9I30^[5]

This report provide wind tunnel test over several symmetrical fuselage models. The fuselage has a uniform cross section in the form of circular cross section. If the fuselage length denoted as L and the fuselage diameter at any fuselage station x denoted as $D(x)$. This NACA report introduced that the distribution of fuselage diameter in the longitudinal axis $D(x)$ is given as^[6]:

$$\mathbf{D}(\mathbf{x}) = \begin{cases} D_m - 2a(x_m - \mathbf{x})^2 & \text{for } 0 \leq x \leq x_m \\ D_m - 2b(x_m - \mathbf{x})^2 & \text{for } x_m \leq x \leq L \end{cases} \quad (2.1)$$

In above equation, the variable a , b and x_m are called as shape parameter. There are 12 fuselage models that had been generated and tested in the wind tunnel. All 12 fuselages have common frontal area $\left(\frac{\pi}{4} D_m^2\right)$ that was equal to 0.307 square foot and base area was 0.0586 square foot. In addition to this, the fineness ratio F_N which represent the ratio of length L to the maximum diameter D had been set for 12.5, 8.91 and 6.04. The fineness ratio $F_N = 12.5$ will correspond with the fuselage length $L = 93.72$ inch, and for $F_N = 8.91$ with fuselage length $L = 66.81$ inch while for $F_N = 6.04$ with fuselage length $L = 45.32$ inch. The shape parameters a , b and x_m for those 12 fuselages are shown in the Table 2.2 below

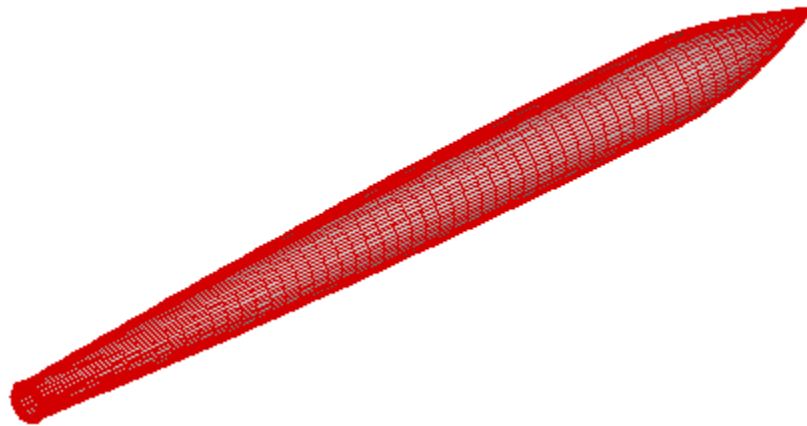
Table 2.2: Parameter fuselage geometry of fuselage model NACA RM 19I30

The body-shape parameters, a and b , have the values given below

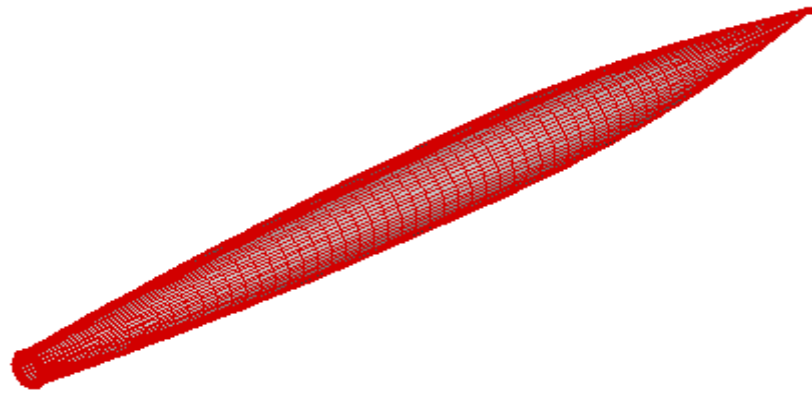
| Configuration | Fineness ratio | K | a | b |
|---------------|----------------|------|----------|----------|
| 1 | 12.5 | 0.20 | 0.010673 | 0.000375 |
| 2 | 12.5 | .40 | .002668 | .000667 |
| 3 | 12.5 | .60 | .001186 | .001501 |
| 4 | 12.5 | .80 | .000667 | .006006 |
| 5 | 8.91 | .20 | .021004 | .000739 |
| 6 | 8.91 | .40 | .005251 | .001313 |
| 7 | 8.91 | .60 | .002334 | .002954 |
| 8 | 8.91 | .80 | .001313 | .011818 |
| a9 | 6.04 | .20 | .04564 | .00161 |
| a10 | 6.04 | .40 | .01141 | .00285 |
| a11 | 6.04 | .60 | .00507 | .00642 |
| 12 | 6.04 | .80 | .00285 | .02563 |

^aConfiguration taken from reference 1.

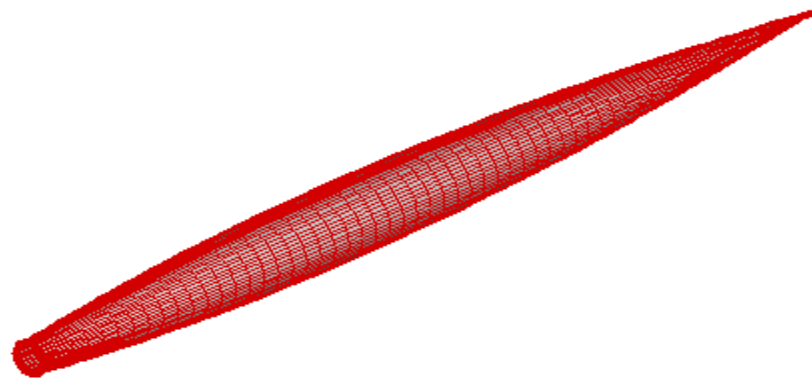
To distinguish with others fuselage shape, the fuselage which developed by use of mathematical expression as given in the Report NACA RM L9I30 denoted as Fuselage RML39I30-J, $J=1,2,3,\dots,12$. Here $J=1$ means that the fuselage generated based on the use of fuselage shape parameter as given in the j^{th} row of the Table 2.2. The shape of fuselage created by use of Eq.2.1, for a given a fixed fineness ratio $F_N = 12.5$ with different location maximum fuselage diameter $x_M = 0.2L, 0.4L, 0.6L$ and $0.8L$ are shown in the Figure 2.2 respectively. While in view for different value of fineness ratio but having the same position of the maximum fuselage diameter for those three value of fineness ratio $F_N = 12.5, 8.91$ and $F_N = 6.04$ are shown in the Figure 2.3 respectively.



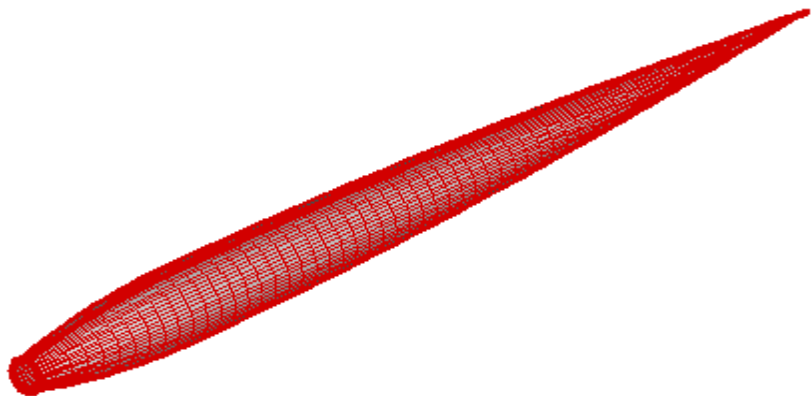
(a)



(b)

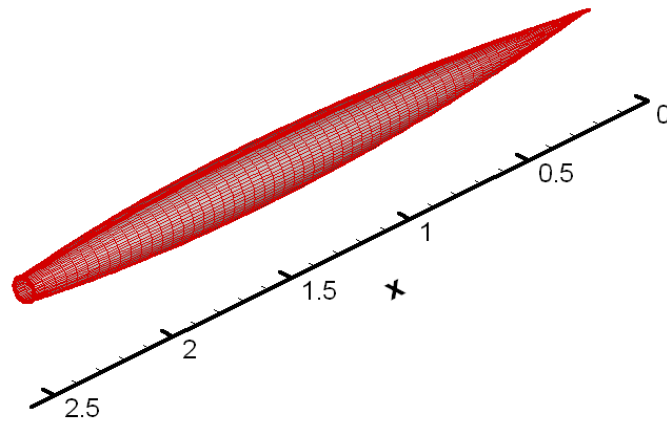


(c)

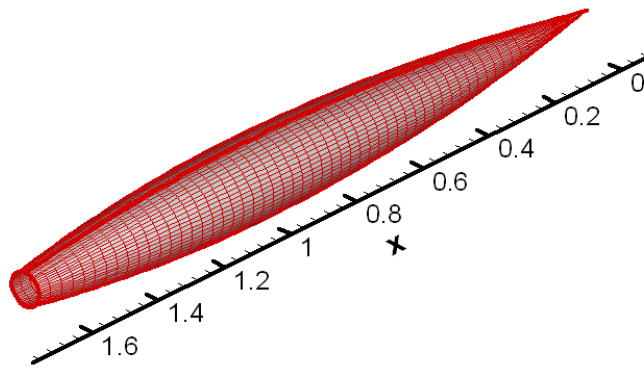


(d)

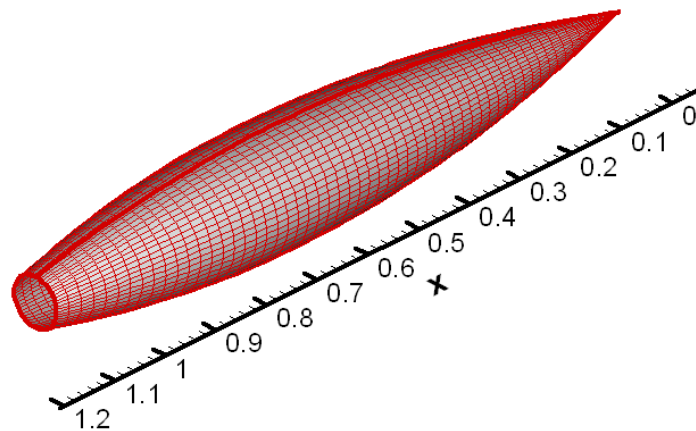
Figure 2.2: Fuselage model RML9I30-1 Fineness ratio $F_N = 12.5$, with (a) $X_M = 0.2L$. (b) $X_M = 0.4L$, (c) $X_M = 0.6L$ and (d) $X_M = 0.8L$



(a)



(b)



(c)

Figure 2.3: Fuselage RML9I30-1 with position maximum diameter $X_M = 0.6L$ and different Fineness ratio. (a) $F_N = 12.5$, (b) $F_N = 8.91$ and (c) $F_N = 6.04$

2.1.2 Symmetrical Fuselage Geometry Model NACA RM A50K24b^[6]

The fuselage geometry was taken from NACA Report RM A50K24b^[7]. This NACA report represent the experimental aerodynamics works on wing body configuration models. The wing plan form is in the form of triangular wing which known as delta wing. The fuselage model having circular cross section, with the distribution of the fuselage radius of the cross section $r(x)$ is given as:

$$r(x) = r_0 \left[1.0 - \left(1.0 - \frac{2x}{L} \right)^2 \right]^{3/4}, \quad 0.0 \leq x \leq L_B \quad (2.2)$$

In above equation r_0 is the maximum fuselage radius cross section, L_B is the actual fuselage length and L is the mathematical fuselage length. Similar equation as given by Eq. 2.2 is also used by other researchers but with different fuselage shape parameters. Table 2.3 shows the value of fuselage shape parameters had been used to generate fuselage as reported in the NACA report.

Table 2.3: The List of NACA Report adopted Fuselage Model RM A50K24b

| No | Source | R_0 (inch) | L_B (inch) | L (inch) |
|----|------------------------------------|--------------|--------------|------------|
| 1 | NACA RM A50K24b ^[6,7,8] | 2.17 | 45.38 | 54.13 |
| 2 | NACA RM A50K20 ^[9] | 3.06 | 60.44 | 76.50 |
| 3 | NACA RM A50K21 ^[10] | 3.06 | 60.44 | 76.50 |
| 4 | NACA RM A9D25 ^[11] | 3.06 | 60.44 | 76.50 |

The top view of the technical drawing of wing body configuration which using Eq. 2.2 for defining the fuselage shape adopted from the Report NACA RM A50K24b as shown in the Figure 2.4

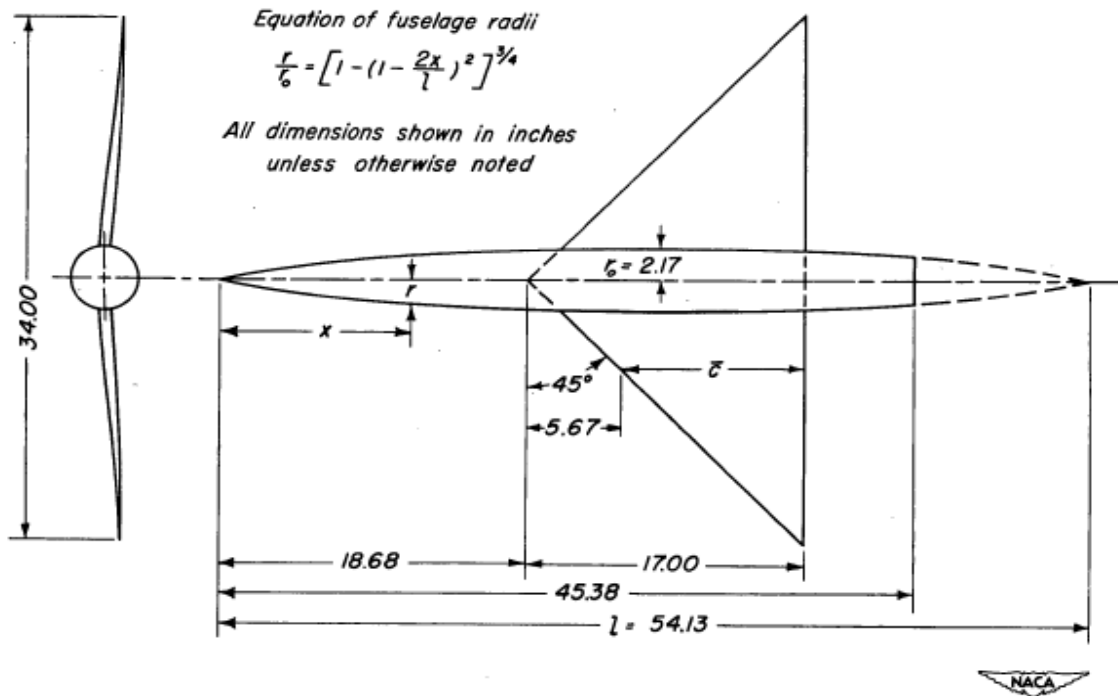
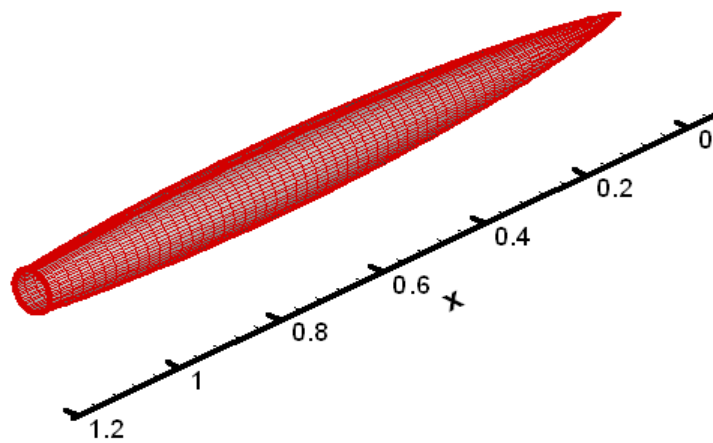
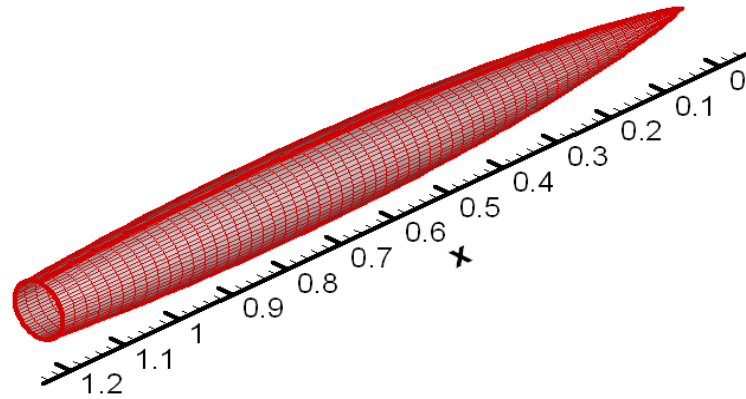


Figure 2.4: The top view of wing body configuration with fuselage shape according to Eq. 2.2^[7]

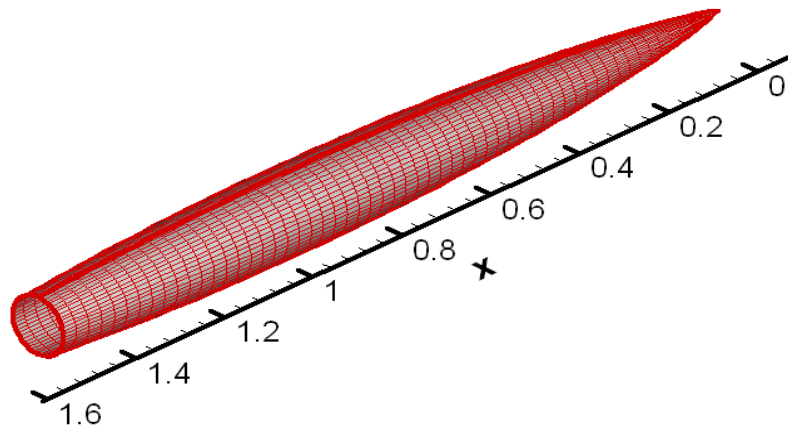
Three dimensional view for those three type of fuselage due to different value of fuselage shape factors as defining their values in the Table 2.3 are shown in the Figure 2.5.



(a)



(b)



(c)

Figure 2.5: Fuselage Model RM A50K24b

2.1.3 Symmetrical Fuselage: Agard's Model – 1 ^[12]

Another mathematical expression to define fuselage shape is using a mathematical model introduced by AGARD ^[12]. For the purpose of wind tunnel calibration, AGARD, tested a body tail configuration as depicted in the Figure 2.6 below:

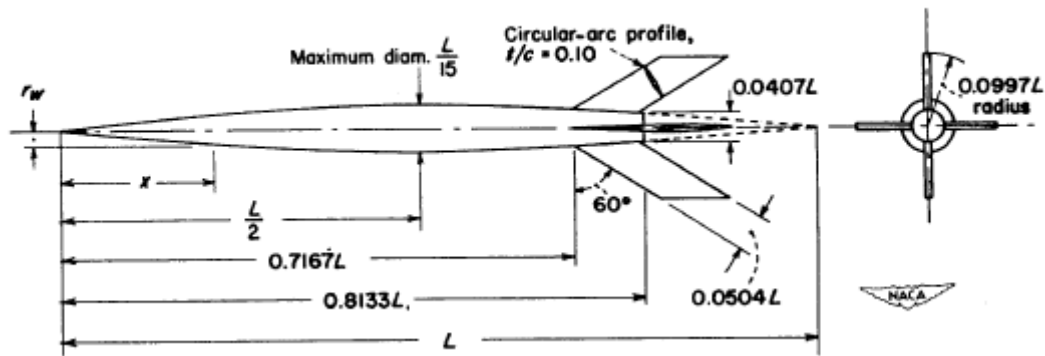


Figure 2.6: The Tail Body Configuration of AGARD Model^[12]

This AGARD model have a circular cross section with the fuselage radius distribution $r(x)$ is defined as:

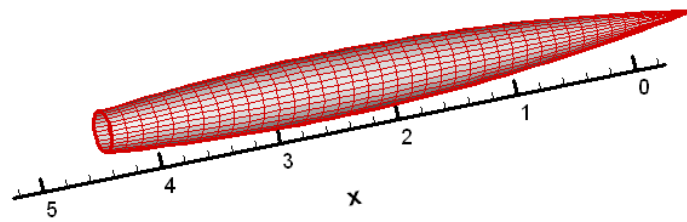
$$r(x) = \frac{x}{7.5} r_0 \left(1 - \frac{x}{L} \right) ; \quad 0.0 \leq x \leq L_B \quad (2.3)$$

Fuselage shape parameters in above equation are the actual fuselage length L_B and the mathematical fuselage length L . Unfortunately in their report, the value for those two shape parameters were not mentioned. However above equation is similar with the equation that had been used to define the NACA RM-10 missile^[13], which the actual fuselage length L_B is set equal to 81.33% of the mathematical fuselage length L . The NACA RM -10 M had been tested in various size of wind tunnel, as result there are various size of RM-10 that had been built. The table 2.4 shows the two fuselage shape parameter that were used to define and built NACA RM-10 missiles in relation with the size of wind tunnel test section where the aerodynamic experiment was conducted.

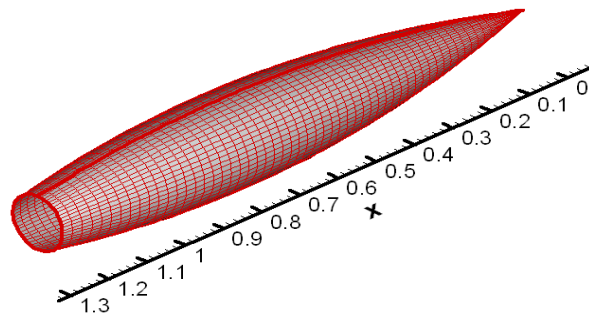
Table 2.4: The actual fuselage length of RM-10 missile related with the size of wind tunnel test section^[13,14,15,16,17]

| No | Wind Tunnel Size of Test Section | L_B (inch) | L |
|----|----------------------------------|--------------|--------|
| 1 | 8 x 6 foot | 73 | 89.76 |
| 2 | 8 x 6 foot | 50 | 61.48 |
| | | 42.05 | 51.70 |
| 3 | 1 x 3 foot | 12.208 | 15.01 |
| 4 | 9 inch | 9 | 11.06 |
| | | 7.325 | 9.006 |
| 5 | Flight | 146.5 | 180.13 |

Figure 2.7(a) shows a three dimensional fuselage shape generated by using Eq. 2.3 for a given $L_B = 0.8133 L = 50$ inches and Figure 2.7(b) for the actual fuselage length $L_B = 7.325$ inches.



(a)



(b)

Figure 2.7: Agard Fuselage Model (a) Fuselage length $L_B = 50$ inches and (b) $L_B = 7.325$ inches

2.1.4 Symmetrical Fuselage: Parabolic Spindle Fuselage model ^[17]

A parabolic spindle Fuselage model having a distribution fuselage radius cross section along the main axis is given as:

$$\frac{r(x)}{L} = 4 \frac{r_{\text{mid}}}{L} \frac{x}{L} \left(1 - \frac{x}{L}\right) \quad (2.4)$$

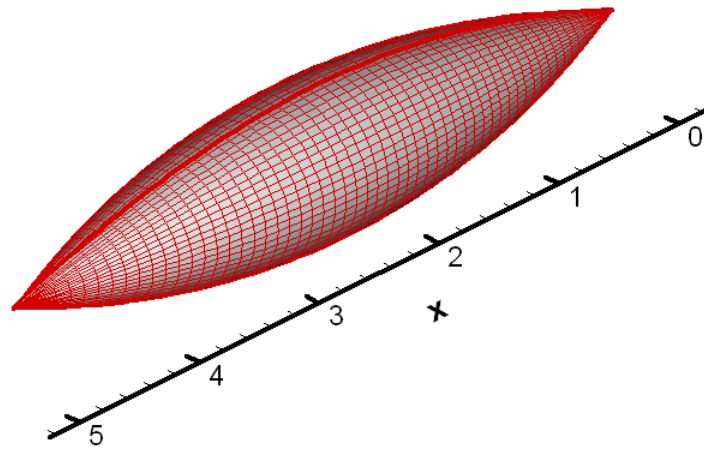
In above equation r_{mid} represents the fuselage radius cross section at the mid fuselage length. It also represents the maximum value of fuselage radius cross section. By definition, fuselage fineness ratio is defined as:

$$F_N = \frac{L}{D_{\text{max}}} = \frac{L}{2 r_{\text{max}}} = \frac{L}{2 r_{\text{mid}}}$$

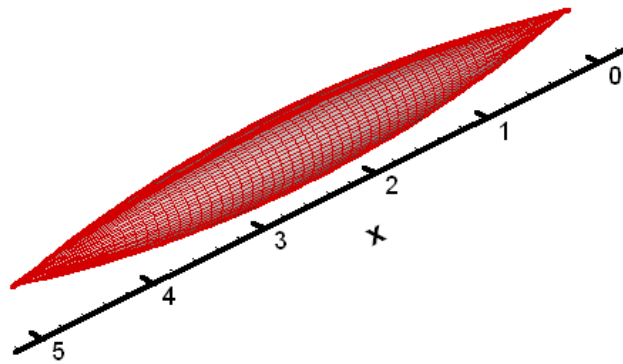
So in term of Fineness ratio F_N above equation, Eq. 2.4, can be written as:

$$\begin{aligned} \frac{r(x)}{L} &= 4 \frac{r_{\text{mid}}}{L} \frac{x}{L} \left(1 - \frac{x}{L}\right) = \frac{2}{L / (2r_{\text{mid}})} \frac{x}{L} \left(1 - \frac{x}{L}\right) \\ &= \frac{2}{F_N} \frac{x}{L} \left(1 - \frac{x}{L}\right) \end{aligned} \quad (2.5)$$

Figure 2.8 shows the three dimensional view of two fuselage models generated by using Eq. 2.5, with the same fuselage length of 5 unit length but differ in term of their fineness ratio. The first figure describes the fuselage geometry for fineness ratio $F_N = 5$, while the second figure for the fineness ratio of 10.



(a)



(b)

Figure 2.8: Parabolic Spindle Fuselage Model (a) Fineness ratio $F_N = 5$, (b) $F_N = 10$

2.1.5 Symmetrical Fuselage: Ellipsoid of revolution ^[17]

The radius of fuselage cross section $r(x)$ for this type of fuselage as:

$$\frac{r(x)}{L} = 2 \frac{r_{\text{mid}}}{L} \sqrt{\frac{x}{L} \left(1 - \frac{x}{L}\right)} \quad (2.6)$$

Here r_{mid} represent the radius of fuselage cross section at the mid length of fuselage. The radius of fuselage cross section at this position is maximum. Hence the fuselage fineness ratio is determined by the r_{mid} . For a given fuselage length L and the fuselage fineness ratio F_N , the radius of fuselage cross section at the mid of fuselage length is

$$r_{\text{mid}} = \frac{L}{2F_N}$$

Figure 2.9 shows two fuselage models created by use of Eq. 2.6. Both fuselages have the same fuselage length L equal to 5 unit length. The first figure correspond to the fuselage with fineness ratio 5 while the second one with $F_N = 10$.

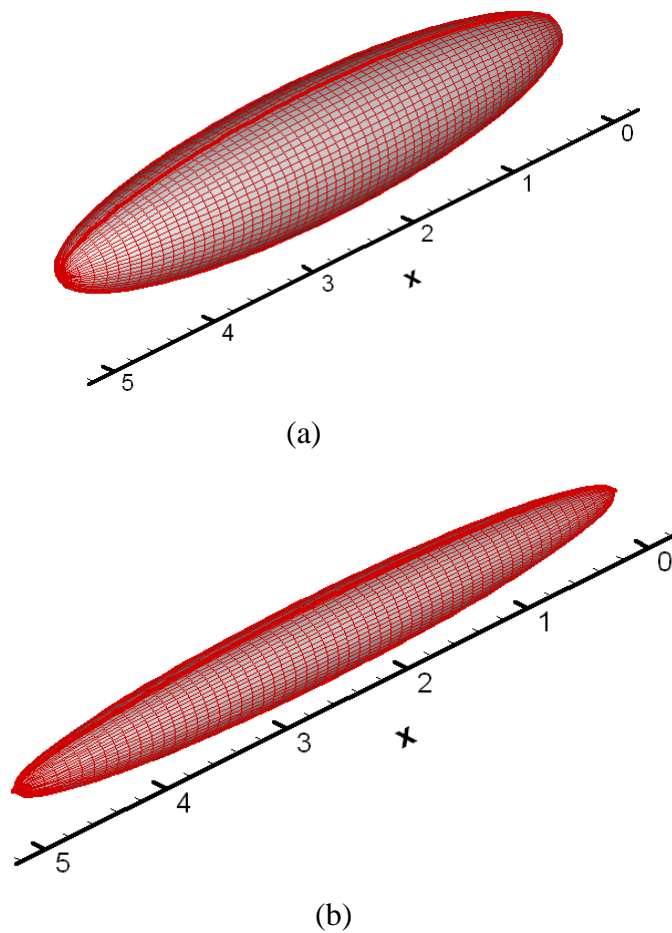


Figure 2.9: Ellipsoidal Fuselage Model (a) Fineness ratio $F_N = 5$, (b) $F_N = 10$

2.2 Mathematical Model for Generating Symmetrical Fuselages: Multi Segments

Due to payload requirements or due to pilot visual ability over the outside environment of the cockpit, the fuselage need to be designed with fuselage partition. The fuselage need to be divided into nose part, fuselage mid section and with addition of fuselage boat tail.

An example of fuselage model which consist of two section, nose part and the fuselage mid section is AGARD model 2^[12]. Other name of Agard model 2 is AGARD model B^[20, 21]. This model actually consist of a wing and body combination. The wing is a delta in the form of an equilateral triangle with a span four times of the body diameter. The body is a cylindrical body of revolution with an Ogive nose. Figure 2.10 is a sketch of the model with the pertinent dimensions given in terms of the body diameter D . This fuselage model had been used for model of wind tunnel calibrations.

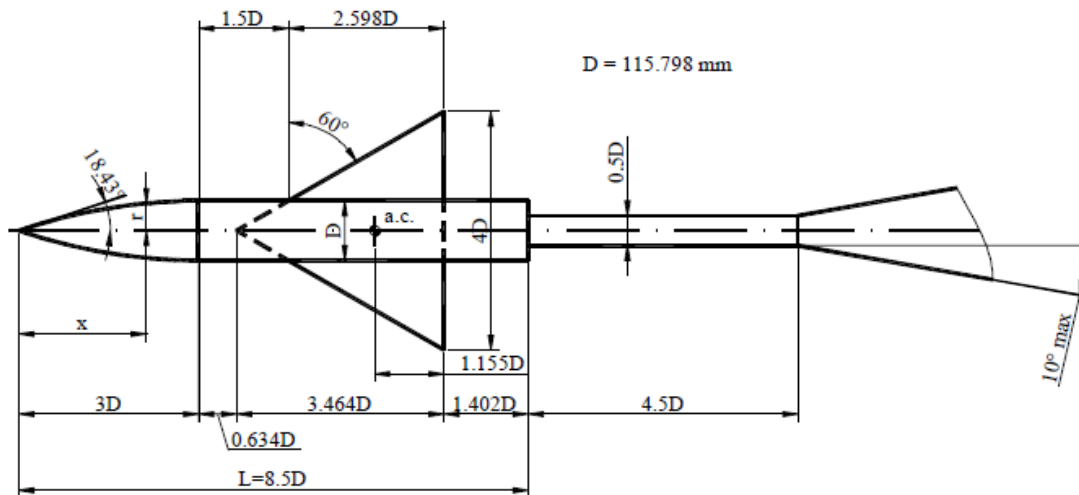


Figure 2.10: Basic Dimension of AGARD Model – B^[12]

The distribution of fuselage radius of cross section for this AGARD model B can be given as:

$$r(x) = \begin{cases} \frac{x}{\ell_N} \left(1 - \frac{1}{(\ell_N)^2} \left(\frac{x}{D} \right)^2 + \frac{1}{2(\ell_N)^3} \left(\frac{x}{D} \right)^3 \right); & x \leq \ell_N D \\ \frac{1}{2} D; & \ell_N D < x \leq L \end{cases} \quad (2.7)$$

In above equation, ℓ_N is nose length factor. Figure 2.10 shows the case of AGARD model – B with nose length factor $\ell_N = 3D$ and the fuselage diameter at the mid section $D = 115.798$ mm. While for a given Fuselage diameter $D = 1.25$ inch, the distribution of fuselage radius cross section of the nose part as given in the Table 2.5 below:

Table 2.5: Nose ordinates of AGARD Model 2^[12]

| Nose ordinates | |
|----------------|--------|
| x, in. | r, in. |
| 0 | 0 |
| .188 | .063 |
| .375 | .124 |
| .563 | .184 |
| .750 | .241 |
| .938 | .296 |
| 1.125 | .343 |
| 1.313 | .394 |
| 1.500 | .436 |
| 1.688 | .475 |
| 1.875 | .508 |
| 2.063 | .537 |
| 2.250 | .561 |
| 2.438 | .580 |
| 2.625 | .599 |
| 2.813 | .608 |
| 3.000 | .616 |
| 3.188 | .621 |
| 3.375 | .623 |
| 3.563 | .624 |
| 3.750 | .625 |

REFERENCES

1. Hoak D.,E et.,al. *USAF Stability and Control Datcom*, McDonnell Douglas Corp., Revised Ed., 1978 .
2. Ellison D.E., et al. *USAF Stability and Control Datcom*, McDonnell Douglas Corp., Revised Ed., 1965.
3. Wolowicz, Chester H, Yancey and Roxanah B. *Longitudinal Aerodynamics Characteristics of Light, Twin Propeller Driven Airplanes*, NASA TN D-6800, 1972.
4. Parks . J.H. *Transonic longitudinal Aerodynamics Effects of Sweeping Up the Rear of the Fuselage of a Rocket Propelled Airplane Model Having No Horizontal Tail “*, NACA RM L54KL2, 1955.
5. Hart, Roger G., Katz, Ellis R. *Flight Investigations At High-Subsonic, Transonic, And Supersonic Speeds To Determine Zero-Lift Drag Of Fin-Stabilized Bodies of Revolution Having Fineness Ratios of 12.5, 8.91, and 6.04 and Varying Positions of Maximum Diameter*, NACA RM, 1949.
6. E. Ray Phelps, Willard G. Smith. *Lift, Drag, And Pitching Moment of Low-Aspect-Ratio Wings At Subsonic and Supersonic Speeds: Triangular Wing of Aspect Ratio 4 With NACA 0005-63 Thickness Distribution, Cambered and Twisted for Trapezoidal Span Load Distribution*, NACA RM A50K24b, 1951.
7. Henry C. Lessing. *Aerodynamic Study of a Wing-Fuselage Combination Employing a Wing Swept Back 63 Degrees: Effect of Sideslip on Aerodynamic Characteristics at a Mach Number of 1.4 with The Wing Twisted and Cambered*, NACA-RM-A50F09; Sep 1950.
8. John C. Heitmeyer. *Aerodynamic Study of a Wing-Fuselage Combination Employing a Wing Swept Back 63 Degrees: Effect of Reynolds Number at Supersonic Mach Numbers on the Longitudinal Characteristics of a Wing Twisted and Cambered for Uniform Load*, NACA-RM-A50G10; Oct 1950.

9. Smith, D.W and Heitmeyer, J.C C. *Lift, Drag, and Pitching Moment of Low-Aspect-Ratio Wings at Subsonic and Supersonic Speeds : Plane Triangular Wing of Aspect Ratio 2 With NACA 0008-63 Section*, NACA RM A50K20.
10. Donald W. Smith, John C. Heitmeyer. *Lift, Drag, and Pitching Moment Of Low-Aspect-Ratio Wings at Subsonic and Supersonic Speeds: Plane Triangular Wing of Aspect Ratio 2 With NACA 0005-63 Section*, NACA RM A50K21, 1951.
11. J. Lloyd Jones, Fred A. Demele. *Aerodynamic Study of A Wing-Fuselage Combination Employing A Wing Swept Back 63 Deg - Characteristics Throughout The Subsonic Speed Range With The Wing Cambered And Twisted for A Uniform Load at a Lift Coefficient Of 0.25*, NACA RM A9D25, 1949.
12. AGARD Memorandum AG 4, Paris. *Specification for Agard Wind Tunnel Calibration Models*, 1955.
13. Edward W. Perkins, Forrest E. Gowen, Leland H. Jorgensen, *Aerodynamic Characteristics of The NACA RM-10 Research Missile in The Ames 1- By 3- Foot Supersonic Wind Tunnel No. 2 : Pressure and Force Measurements at Mach Numbers Of 1.52 and 1.98*, NACA-RM-A51G13; Sep 1951.
14. Hoffman, Sherwood. *Free-Flight Tests To Determine The Power-On and Power-Off Pressure Distribution and Drag Of The NACA RM-10 Research Vehicle at Large Reynolds Numbers Between Mach Numbers 0.8 and 3.0*; NACA-RM-L55H02; September 20, 1955.
15. Albert J. Evans. *The Zero-Lift Drag Of A Slender Body of Revolution (NACA RM-10 Research Model) As Determined From Tests In Several Wind Tunnels and In Flight At Supersonic Speeds*; Naca-Report-1160; 1954.
16. Piland, Robert O. *Drag Measurements on A 1/6-Scale, Finless, Sting-Mounted NACA RM-10 Missile In Flight At Mach Numbers From 1.1 to 4.04 Showing Some Reynolds Number and Heating Effects*; NACA-RM-L54H09; October 27, 1954.
17. Krasnov, N.F. *Aerodynamics of Bodies of Revolution* edited and annotated by D.N. Morris, American Elsevier, New York, 1970.
18. Evan, A.J. *The Zero Lift Drag of A Slender Body of Revolution (NACA RM – 10 Research Model) as Determined From Tests In Several Wind Tunnels and In Flight at Supersonic Speeds*, NACA Report 1160.

19. Adam M.C. *Determination of Shapes of Boattail Bodies of Revolution for Minimum Wave Drag*, NACA TN 2550, 1951.
20. Lighthill M.J. *Supersonic Flow Past Bodies of Revolution*, R & M No 2003 British A.R.C., 1945.
21. Schueler, C.J. *AGARD Tests – Comparison of Wind Tunnel and Free Flight Results*, Huntsville, Alabama, 1957.
22. Schueler, C.J. *Comparison of the Aerodynamics Characteristics of AGARD Model A from Tests in 12 inc and 40 inch Supersonic Wind Tunnels*, Arnold Engineering Development Center , AEDC-TN-61-8, 1961.
23. Gapcynski, J.P. R and, Warner A. *The Effect of Nose Radius and Shape on the Aerodynamic Characteristics of A Fuselage and A Wing-Fuselage Combination at Angles Of Attack “*, NACA RM L53I23A, 1953.
24. Robert Lauren Acker. *Determination of the Nose Cone Shape for a Large Reusable Liquid Rocket Booster*, Massachusetts Institute of Technology, 1987
25. Ashley.H, Landahl,M., *Aerodynamics of Wings and Bodies*, Addison-Wesley, 1965.
26. E. Proyono, Lavi R. Zuhail and H. Djohodiharjo. *Numerical Study of Shock Generation at the Aftbody of Slender Body of Revolution Using Navier-Stokes Equation*, ITB, 2002
27. <http://www.fiddlersgreen.net/models/aircraft/ASW20-sailplane.html>
28. <http://www.aircav.com/recog/chp08/ch08aclist/c-130.html>
29. http://www.aviationexplorer.com/727_facts.htm
30. Park J.H. *Transonic Longitudinal Aerodynamics Effects of Sweeping up the Rear of the Fuselage of a Rocket Propelled Airplane Model Having No Horizontal Tail*, NACA RM L54K12, 1955.
31. Park.J.H and Kehlet A.B. *Longitudinal Stability and Trim of Two Rocket Propelled Airplane Models of an Airplane Configuration Having a 45⁰ Sweptback Wings and Unswept Horizontal Tail*, NACA RM L52F05, 1952.
32. Park.J.H and Kehlet A.B. *Longitudinal Stability and Trim of Two Rocket Propelled Airplane Models Having 45⁰ Sweptback Wings and Tails with the Horizontal Tail Mounted in Two Positions*, NACA RM L53JL2A, 1953.
33. Ladson C.L, Brooks C.W, Hill, A.S. and Sproles D.W. *Computer Program to Obtain Ordinates for NACA Airfoils*, NASA TM 4741, 1996.

34. Abbott, I.H., and von Doenhoff, A.E. *Theory of Wing Sections*, Dover publications, Inc. New York, 1958.
35. Jacobs E.N, Ward K. E, and Pinkerton, R.M. *The Characteristics Of 78 Related Airfoil Sections From Tests In The Variable-Density Wind Tunnel*, NACA Report No. 460, 1933.
36. Allen, H. Julian and Perkins, Edward W. *Characteristics of Flow over Inclined Bodies of Revolution*, NACA RM A50L07, 1951.
37. Roskam, J. and Lan, C.T. *Airplane Aerodynamics and Performance*, DARcorporation, USA, 1997
38. Jim Upton, *Lockheed L-1011 Tristar*, ISBN, 158007037X, 9781580070379, 2001
39. Masson W.H. *Appendix A Geometry for Aerodynamicists*, VPI, 2006
40. Edward C. Polhamus. *Effect of Flow Incidence and Reynolds Number on Low-Speed Aerodynamic Characteristics of Several Noncircular Cylinders with Applications to Directional Stability and Spinning*, NACA TN 4176, 1958.
41. Sherman A. *Interference of Wing and Fuselage from Tests of 30 Combinations with Triangular and Elliptical Fuselage in the NACA Variable Density Tunnel*, NACA TN 1276, 1947.
42. Jacobs E.N. and Ward K.E. *Interference of Wing and Fuselage from Tests of 209 Combinations in the NACA Variable Density Tunnel*, NACA Rep. 540.
43. Letko W. *Experimental Investigation At A Mach Number Of 3.11 Of The Lift, Drag, And Pitching-Moment Characteristics Of Five Blunt Lifting Bodies*, NASA TN D-226,1960.
44. William Letko; Edward C B Danforth. *Theoretical Investigation at Subsonic Speeds of the Flow Ahead Of a Slender Inclined Parabolic-Arc Body of Revolution and Correlation with Experimental Data Obtained at Low Speeds*, NACA TN 3205, 1954.
45. Letko W., and Williams J.L. *Experimental Investigation At Low Speed Of Effects Of Fuselage Cross Section On Static Longitudinal And Lateral Stability Characteristics Of Models Having 0 And 45 Degrees Sweptback Surfaces*, NACA TN 3551, 1955.
46. 2000-2010, *FAA General Aviation and Air Taxi Activity (and Avionics) Surveys*
47. 2010 *General Aviation Statistical Databook & Industry Outlook*.

48. Pasquale M. Sforza, *Commercial Airplane Design Principles, Chapter 3, Fuselage Design* 47 – 79, 2014
49. A. Da Ronch, M. Ghoreyshi, K.J. Badcock. *On the Generation of Flight Dynamic Aerodynamic Tables by Computational Fluid Dynamics*, Progress in Aerospace Science 47, 2011
50. Y. K. Wang, S. Ou, X. Y. Deng, J. Wen. *Effect of Vortex Generator on Lateral and Directional Aerodynamic Characteristic at Medium Angle of Attack*, Procedia Engineering 67, 2013
51. Joseph A. Schetz, Serhat Hosder, Vance Dippold, Jessica Walker. *Propulsion and Aerodynamic Performance Evaluation of Jet Wing Distributed Propulsion*, Aerospace Science and Technology, 2010
52. Dong Sun, Huaiyu Wu, Chi Ming Lam, Rong Zhu. *Development of a Small Air Vehicle Based on Aerodynamic Model Analysis in the Tunnel Tests*, Mechatronics, 2006
53. Mark Drela and Michael B. Giles. *Viscous-Inviscid of Transonic and Low Reynolds Number Airfoils*, AIAA Journal, 25(10):1347-1355, Oct 1987
54. Boermans L.L.M., and Nicolosi F. “*Sailplane Fuselage and Wing-Fuselage Junction Design*”, XXV Ostiv Congress - S. Auban, France, 3-11 July 1997
55. Brunello D., Clarke G. And Reddy R. “*Numerical and Experimental Analysis of a Representative ADF Helicopter Fuselage*”, 28th International Congress Of The Aeronautical Sciences, ICAS , 2012
56. Kusyumov A.N, Mikhailov S.A, Garipov A.O., Nikolaev E.I. and G. Barakos. “*Simulation of Fuselage Aerodynamics of the ANSAT Helicopter Prototype*” Transaction on Control and Mechanical System, Vol. 1. No. 7. Pp 318-324, Nov. 2012
57. Bento Silva de Mattos. “*Aircraft Design Configuration*”, Brazil, December, 2008
58. Bento Silva de Mattos. “*Fuselage Design*”, ITA, Brazil, 2009
59. Armes R.J. “*Aerodynamic Fuselage Design and Engine Integration for the Vampire Light Sport Aircraft*” Ms. Thesis, Aerospace Engineering, North Carolina State University, 2013